PARAMETER ESTIMATION OF MULTIPLE POLES BY SUBSPACE-BASED METHODS

Prabhu Vijayan[⋆†] *Mariya Ishteva*[⋆] *Ivan Markovsky*[‡]

[⋆]KU Leuven, Campus Geel, Department of Computer Science, 2440 Geel, Belgium.
[†]Vrije Universiteit Brussel, Department ELEC, Pleinlaan 2, 1050 Brussel, Belgium.
[‡]Catalan Institution for Research and Advanced Studies (ICREA), Barcelona, Spain and
The International Centre for Numerical Methods in Engineering (CIMNE), Barcelona, Spain.

ABSTRACT

This work deals with the problem of estimating model parameters (model order, pole multiplicity, frequency, damping factor, amplitude and phase) of exponential polynomials. We introduce a general signal model, containing multiple poles, and show, why and how this generalization is true algebraically for the general class of signals. Poles estimation methods like Rotational Invariant Technique (RIT), and Hankel Total Least Square (HTLS) method are used. We propose a solution to estimate complex amplitudes using the estimated signal poles. An algorithm to estimate model order and multiplicity associated with it, for any measured signal, is also developed.

keywords: parameter estimation, subspace method, harmonic retrieval, multiple pole, Vandermonde decomposition.

I. INTRODUCTION

In communication and signal processing, retrieval of information from measured data is vital. These data, corrupted by noise, do not enable the prediction of the signal deterministically. Various statistical methods have been used historically. The linear prediction method by Prony [14] and Pisarenko [15] estimates the parameters of sum-of-exponentials (SOE). Some modern estimation techniques are maximum likelihood methods [2], subspace-based methods [4]-[6], [8] and matrix pencil techniques [7]. The backward prediction [3] is a linear method, that differs from using Singular Value Decomposition (SVD). The subspace-based methods like HTLS [8], Kung's realization [10], and RIT [12] are popular for their accuracy of estimation. These methods are suitable for signals, containing simple poles.

The SOE signal finds application in electromagnetic pulse situations to define various pulse waveforms [1]. The aforementioned estimation methods are used to estimate simple poles. However, in practice, there are applications where poles are multiple. A relevant example is the critically damped simple harmonic motion of a spring-mass system, that has a double pole. For such applications, the SOE model needs a generalization. The Polynomial Amplitude Complex Exponentials (PACE) model [12], addresses this issue. This paper presents a general class of signal sequences, that has multiple poles, proposes an algorithm for the estimation of model order, multiplicity and complex amplitudes and shows, how the choice of estimation methods affects the accuracy of estimation. The rationale behind the model proposal is from the theory of differential/difference equations when the characteristic polynomial has repeated roots.

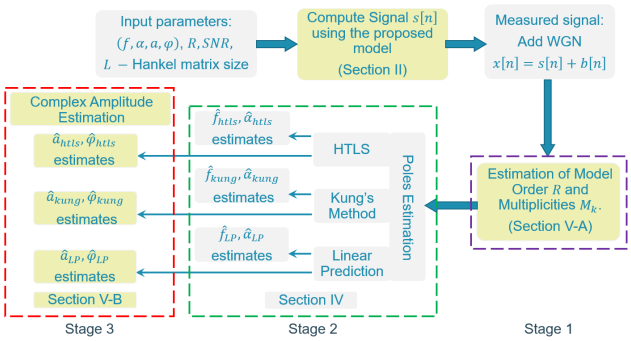

Fig. 1: Outline of the paper - The blocks marked in yellow indicate the original contributions of this work.

The schematic in Fig. 1 explains the parameter estimation procedure, starting from feeding the input parameters to the algorithm and estimating them back in three different stages. In practice, we have the measured signal, contaminated by noise, whose parameters are unknown. The paper is structured as follows: In Section II, we propose a generalized signal model, representing the general class of signals and compare it with the existing model [12]. In Section III, we explain the matrix form of the proposed model and justify the chosen parametrization algebraically. Section IV summarizes various poles estimation techniques given in [8],[10],[3]. We propose a method to estimate model order and multiplicity, in Section V. Further, Section VI presents the influence of Hankel matrix size on estimates and introduces an optimal matrix size for better accuracy. The results of numerical simulation are provided in Section VII, along with a comparison of various estimation methods, and signal models, leading to the conclusions in Section VIII.

II. GENERALIZED SIGNAL MODEL

Here, we propose a generalized signal model, with a polynomial basis function, that can account for the multiple poles and discuss another general model in the literature.

The discrete-time signal, x_n (1), is modelled as a sum of K complex damped exponentials [8], corrupted by white Gaussian noise (WGN) b_n, where $j = \sqrt{-1}$, time index $n = 0, ..., N-1$,N is the number of samples, $K \in \mathbb{N}^*$ is the model order (* cannot be 0) and Δt is the sampling time interval. The parameters defining the model are frequency f_k, damping factor α_k, amplitude a_k and phase ϕ_k.

$$x_n = \sum_{k=1}^{K} (a_k e^{j\phi_k})(e^{\{(-\alpha_k + j2\pi f_k)\Delta t\}n}) + b_n, \tag{1}$$

$$x_n = \sum_{k=1}^{K} c_k z_k^n + b_n, \quad n = 0, 1, ..., N-1, \tag{2}$$

In the compact form (2), $c_k = a_k e^{j\phi_k} \in \mathbb{C}$ and $z_k = e^{(-\alpha_k + j2\pi f_k)\Delta t} \in \mathbb{C}^*$ (* cannot lie on 0 in complex plane) are k^{th} complex amplitude and pole, respectively. Here, z_k's are distinct. The SOE signal x_n in (2), without noise, satisfies the homogeneous recurrence relation of length K (3), as in [3], where $p_1, ..., p_K$ are coefficients of polynomial (4),

$$p_0 x_n + p_1 x_{n-1} + ... + p_K x_{n-K} = 0, \quad p_0 = 1, p_K \neq 0, \tag{3}$$

$$g(u) = \prod_{k=1}^{K} (u - z_k) = \sum_{k=0}^{K} p_{K-k} u^k. \tag{4}$$

The linear prediction method [3], thus predicts the polynomial $g(u)$ from data and the roots of polynomial are the estimated poles. This signal model is restricted to signals containing simple poles, and is not the general solution of homogeneous linear recursion, since a prediction polynomial in the general case can have repeated roots [12]. Thus, (4) is generalized [12], considering the multiplicity of poles as:

$$g(u) = \prod_{k=1}^{r} (u - z_k)^{M_k} = \sum_{k=0}^{R} p_{R-k} u^k. \tag{5}$$

where $M_k \in \mathbb{N}^*$ (* cannot be 0) is poles multiplicity $\forall k = 1, ..., r$, r is number of distinct poles and $R = \sum_{k=1}^{r} M_k$. When poles are simple, then $r = K = R$. The solution to recurrence relation (3), of length R, is obtained by modifying (2) as below, given in [12]:

$$x_n = \sum_{k=1}^{r} c_k(n) z_k^n + b_n, \quad n = 0, 1, ..., N-1, \tag{6}$$

where $c_k(n)$ is a k^{th} complex amplitude, as a polynomial function of time index n and is of order $M_k - 1$. A simple polynomial basis function, that satisfies linear recursion, is adopted from the theory of differential/difference equations for the characteristics polynomial with repeated roots, given in [16]. The complex polynomial $c_k(n)$ is given by:

$$c_k(n) = \sum_{l=1}^{M_k} n^{l-1} \tilde{c}_{kl}, \tag{7}$$

where $\tilde{c}_{kl}$ is a complex amplitude. Thus, the parameterized general signal model for (6) proposed here is:

$$\tilde{x}_n = \sum_{k=1}^{r} \sum_{l=1}^{M_k} n^{l-1} \tilde{c}_{kl} z_k^n + b_n, \quad n = 0, 1, ..., N-1. \tag{8}$$

The parameters of the model to be estimated are order R, pole multiplicity $M_k, k = 1, ..., r$, r signal poles z_k and R complex amplitudes $\tilde{c}_{kl}$. This model is referenced in this paper as a "proposed" model, with $\sim$ representing the associated quantities.

Another particular polynomial basis function, used in [12] for general signal model (6), is parametrized as (9):

$$x'_n = \sum_{k=1}^{r} \sum_{l=1}^{M_k} F_{l-1}(n) c'_{kl} z_k^{n-l+1} + b_n, \quad n = 0, ..., N-1, \tag{9}$$

where c'_{kl} is a complex amplitude and the function $F_{l-1}(n)$ is an $(l-1)^{\text{th}}$ order polynomial, defined as:

$$F_{l-1}(n) = \begin{cases} 1, & \text{if } l = 1 \\ \dfrac{1}{(l-1)!} \displaystyle\prod_{i=0}^{l-2} (n - i), & \text{if } l > 1 \end{cases} \tag{10}$$

The model (9) is referenced in this paper as "PACE", with $'$ representing the associated quantities. The proposed (8) and PACE (9) models differ in their parametrization, (i.e.) their poles are equal, but their complex amplitudes are proportional, as derived in Section V-C.

III. MATRIX MODEL

The matrix form of the proposed model and the algebraic reason behind the parametrization are presented here.

The subspace-based methods [5],[6],[8]-[10] rely on the data matrix structure. They operate on the "Hankel-structured" data matrix $\boldsymbol{H}$, constructed using N data samples of x_n (6). The size of $\boldsymbol{H}$ is $L \times M$ and $\{L, M\} > R$, where L is hyperparameter and $M = N - L + 1$.

$$\boldsymbol{H} = \begin{bmatrix} x_0 & x_1 & \dots & x_{M-1} \\ x_1 & \iddots & \iddots & x_M \\ \vdots & \iddots & \iddots & \vdots \\ x_{L-1} & \dots & x_{N-2} & x_{N-1} \end{bmatrix}$$

The choice of L plays a significant role in the performance of subspace-based methods. A study on this is provided in Section VI. If $rank(\boldsymbol{H}) < \min(L, M)$, signal x_n satisfies the model (8) exactly. For signal sequence (8) without noise,

$\boldsymbol{H}$ admits generalized Vandermonde decomposition (11), that is used to estimate complex amplitudes $\hat{c}_k$ and poles $\hat{z}_k, k = 1, 2, ..., K$, where $\boldsymbol{D}$ is $R \times R$ block-diagonal matrix, with each block size corresponding to their multiplicities.

$$\boldsymbol{H} = \boldsymbol{T}_L \boldsymbol{D} \boldsymbol{T}_M^T, \tag{11}$$

$$\boldsymbol{D}_k = \begin{bmatrix} \tilde{c}_{k1} & \tilde{c}_{k2} & \tilde{c}_{k3} & \tilde{c}_{k4} & \dots & \tilde{c}_{kM_k} \\ \tilde{c}_{k2} & 2\tilde{c}_{k3} & 3\tilde{c}_{k4} & \iddots & \iddots & \\ \tilde{c}_{k3} & 3\tilde{c}_{k4} & \iddots & \iddots & & \\ \tilde{c}_{k4} & \iddots & \iddots & & & \\ \vdots & \iddots & & & & \\ \tilde{c}_{kM_k} & & & & & \end{bmatrix},$$

$$\boldsymbol{D}_k = \begin{cases} \binom{i+j}{i} \tilde{c}_{kl} & = \dfrac{(i+j)!\tilde{c}_{kl}}{i!j!}, \\ & \text{if } i+j \leq M_k - 1, \\ 0, & \text{otherwise}, \end{cases} \tag{12}$$

The block k is $M_k \times M_k$ anti upper-triangular Pascal matrix, $\forall\ k \in [1, ..., r]$ and $l \in [1, ..., M_k]$, $i, j = 0, ..., M_k - 1$, are local positional indices. $\boldsymbol{T}_L$ and $\boldsymbol{T}_M$ are modified-confluent Vandermonde matrices of sizes $L \times R$ and, $M \times R$:

$$\boldsymbol{T} = \begin{bmatrix} \begin{bmatrix} \hat{z}_1^n \\ n\hat{z}_1^n \\ n^2\hat{z}_1^n \\ \vdots \\ n^{M_1-1}\hat{z}_1^n \end{bmatrix}^T & \dots & \begin{bmatrix} \hat{z}_r^n \\ n\hat{z}_r^n \\ n^2\hat{z}_r^n \\ \vdots \\ n^{M_r-1}\hat{z}_r^n \end{bmatrix}^T \end{bmatrix},$$

where $n = 0, ..., L$ and $n = 0, ..., M$ for $\boldsymbol{T}_L$ and $\boldsymbol{T}_M$ respectively, $\hat{z}_1, ...\hat{z}_r$ are estimated poles. The subscript r indicates the number of distinct poles, and $M_1, ..., M_r$ are the multiplicities of the r distinct poles. The parameters are then indirectly estimated by exploiting the shift-invariance property of $\boldsymbol{T}$, in [9] (also true for multiple poles), where $\boldsymbol{T}_\uparrow$ and $\boldsymbol{T}_\downarrow$ are matrices formed by removing the first and last row of $\boldsymbol{T}$ respectively. $\boldsymbol{Z}$ is a $R \times R$ block-diagonal matrix, with each block size equal to their multiplicities.

$$\boldsymbol{T}_\uparrow = \boldsymbol{T}_\downarrow \boldsymbol{Z}, \tag{13}$$

The block k is an $M_k \times M_k$ upper triangular Pascal matrix,

$$\boldsymbol{Z}_k = \begin{bmatrix} \hat{z}_k & \hat{z}_k & \hat{z}_k & \hat{z}_k & \dots & \hat{z}_k \\ & \hat{z}_k & 2\hat{z}_k & 3\hat{z}_k & \dots & \vdots \\ & & \hat{z}_k & 3\hat{z}_k & \dots & \vdots \\ & & & \hat{z}_k & \ddots & \vdots \\ & & & & \ddots & \vdots \\ & & & & & \hat{z}_k \end{bmatrix},$$

$$\boldsymbol{Z}_k = \begin{cases} \binom{j}{i} \hat{z}_k = \dfrac{j!\hat{z}_k}{i!(j-i)!}, & \text{if } i \leq j, \\ 0, & \text{otherwise}, \end{cases} \tag{14}$$

where $i, j = 0, ..., M_k - 1$ are local positional indices of block k. Using SVD of $\boldsymbol{H}$ and equation (13), the poles are estimated with better numerical stability. For the noisy data matrix, the total least square (TLS) method is used [9].

Using an example and the factorization (11), the proposed model is algebraically justified. Let $r = 1, M_1 = 4, R = 4$ and $L = M = 5$, then from (13),

$$\begin{bmatrix} \hat{z}_1 & \hat{z}_1 & \hat{z}_1 & \hat{z}_1 \\ \hat{z}_1^2 & 2\hat{z}_1^2 & 4\hat{z}_1^2 & 8\hat{z}_1^2 \\ \hat{z}_1^3 & 3\hat{z}_1^3 & 9\hat{z}_1^3 & 27\hat{z}_1^3 \\ \hat{z}_1^4 & 4\hat{z}_1^4 & 16\hat{z}_1^4 & 64\hat{z}_1^4 \end{bmatrix} = \begin{bmatrix} 1 & 0 & 0 & 0 \\ \hat{z}_1 & \hat{z}_1 & \hat{z}_1 & \hat{z}_1 \\ \hat{z}_1^2 & 2\hat{z}_1^2 & 4\hat{z}_1^2 & 8\hat{z}_1^2 \\ \hat{z}_1^3 & 3\hat{z}_1^3 & 9\hat{z}_1^3 & 27\hat{z}_1^3 \end{bmatrix} \boldsymbol{Z}, \tag{15}$$

where $\boldsymbol{Z}$ is a 4×4 upper triangular Pascal matrix

$$\boldsymbol{Z} = \begin{bmatrix} \hat{z}_1 & \hat{z}_1 & \hat{z}_1 & \hat{z}_1 \\ & \hat{z}_1 & 2\hat{z}_1 & 3\hat{z}_1 \\ & & \hat{z}_1 & 3\hat{z}_1 \\ & & & \hat{z}_1 \end{bmatrix}.$$

IV. SIGNAL POLES ESTIMATION

This section briefs some existing pole estimation methods.

IV-A. Hankel Total Least Square Method

The rank R truncated SVD of $\boldsymbol{H}$ is $\boldsymbol{H} \approx \boldsymbol{H}_R = \boldsymbol{U}_R \boldsymbol{\Sigma}_R \boldsymbol{V}_R^H$, where $\boldsymbol{U}_R$, $\boldsymbol{V}_R$ are R left, right singular vectors, respectively. $\boldsymbol{\Sigma}_R$ is $R \times R$ singular value matrix. Using shift-invariance property [8], poles are estimated as:

$$\boldsymbol{U}_{R\uparrow} = \boldsymbol{U}_{R\downarrow} \boldsymbol{E}, \tag{16}$$

$\boldsymbol{U}_{R\uparrow}$ and $\boldsymbol{U}_{R\downarrow}$ are formed by removing the first and last row of $\boldsymbol{U}_R$ respectively. Solving (16) by TLS method [8], the eigenvalues of $\boldsymbol{E}$ are the pole estimates $\hat{z}_k$, $k = 1, ..., R$.

IV-B. Kung's Realization Method

In Kung's method [10], the rank revealing factorization $\boldsymbol{H} = \boldsymbol{\Gamma}\boldsymbol{\Delta}$, involves observability $\boldsymbol{\Gamma}$ and controllability $\boldsymbol{\Delta}$ matrices. But this is a nontrivial problem in finite precision arithmetic. Thus, using SVD, the factors are $\boldsymbol{\Gamma} = \boldsymbol{U}_R \sqrt{\boldsymbol{\Sigma}_R}$ and $\boldsymbol{\Delta} = \sqrt{\boldsymbol{\Sigma}_R} \boldsymbol{V}_R^H$. The linear system is solved for $\boldsymbol{E}$,

$$\boldsymbol{\Gamma}_\uparrow \boldsymbol{E} = \boldsymbol{\Gamma}_\downarrow, \tag{17}$$

where $\boldsymbol{\Gamma}_\uparrow$ and $\boldsymbol{\Gamma}_\downarrow$ are sub-matrices of $\boldsymbol{\Gamma}$ with first and last row removed, respectively. The eigenvalues of $\boldsymbol{E}$ are the pole estimates $\hat{z}_k$, $k = 1, ..., R$.

IV-C. Linear Prediction

From the recurrence relation (**??**), the entire signal can be generated, provided the initial R samples $x_0, ..., x_{R-1}$ are known, as given in [3] and [12]. In the system identification problem, the signal sequence x_n is already known. Thus, the recurrence relation is solved for the unknown coefficients

$p_1, ..., p_R$. The recurrence matrix $\boldsymbol{X}$ of size $(N-R) \times R$ and vector $\boldsymbol{x}$ of length $N-R$ are constructed using x_n.

$$\boldsymbol{X} = \begin{bmatrix} x_{R-1} & x_{R-2} & \dots & x_0 \\ x_R & x_{R-1} & \dots & x_1 \\ \vdots & \vdots & \ddots & \vdots \\ x_{N-2} & x_{N-3} & \dots & x_{N-R+1} \end{bmatrix}, \boldsymbol{x} = \begin{bmatrix} x_R \\ x_{R+1} \\ \vdots \\ x_{N-1} \end{bmatrix}.$$

The coefficients $p_1, ..., p_R$ of (**??**) in $\boldsymbol{p}$ are determined by:

$$\boldsymbol{X}\boldsymbol{p} = -\boldsymbol{x}, \tag{18}$$

The $R \times R$ companion matrix $\boldsymbol{A}$ is constructed using $\boldsymbol{p}$,

$$\boldsymbol{A} = \begin{bmatrix} -p_1 & \dots & -p_{K-1} & -p_R \\ 1 & \dots & 0 & 0 \\ \vdots & \ddots & \vdots & \vdots \\ 0 & \dots & 1 & 0 \end{bmatrix}.$$

The characteristic equation of the R^{th} order difference equation (**??**) is given by $\det(\boldsymbol{A} - \lambda \boldsymbol{I}) = 0$,

$$\lambda^R + p_1\lambda^{R-1} + p_2\lambda^{R-2} + ... + p_R = 0. \tag{19}$$

Solving (19), $\hat{z}_k$, $k = 1, ..., R$ are estimated, as in [3], [12].

IV-D. Estimation of Frequency and Damping Factor

Using the poles $\hat{z}_k$, $k = 1, ..., R$ estimated in Sections IV-A - IV-C, the frequency $\hat{f}_k$ and damping factor $\hat{\alpha}_k$ estimates for the k^{th} pole are determined as follows:

$$\hat{z}_k = e^{\{(-\hat{\alpha}_k + j2\pi\hat{f}_k)\Delta t\}}, \tag{20}$$

$$\hat{f}_k = \frac{1}{2\pi\Delta t} \arctan\left(\frac{\Im(\hat{z}_k)}{\Re(\hat{z}_k)}\right), \tag{21}$$

$$\hat{\alpha}_k = \frac{-\log\left(\sqrt{\Re(\hat{z}_k)^2 + \Im(\hat{z}_k)^2}\right)}{\Delta t}, \tag{22}$$

where $\Re(\hat{z}_k)$ and $\Im(\hat{z}_k)$ are real and imaginary parts of $\hat{z}_k$.

V. ESTIMATION OF MODEL ORDER AND COMPLEX AMPLITUDE

This section presents a method to estimate the model order and multiplicities of every individual pole. We also propose a method to estimate complex amplitude for the chosen parametrization (8) and derive the relationship between the PACE (9) and the proposed model.

V-A. Estimation of Model Order and Multiplicities

In the noise-free case, the model order R is equal to $rank(\boldsymbol{H})$, but in practice, the model order R and multiplicities $M_k, k = 1, ..., r$ need to be estimated. The classical Akaike Information Criterion (AIC) is used to estimate the model order, which employs an estimation dataset cost function $V_{est}(n_p)$ and multiplies it with a penalty term for the increasing model order n_p,

$$V_{est}(n_p) = \frac{1}{N\sigma^2}||\tilde{x}_n - \tilde{x}_{est}(n_p)||^2, \tag{23}$$

$$V_{AIC}(n_p) = V_{est}(n_p)\left(1 + \frac{2n_p}{N}\right), \tag{24}$$

where σ^2 is variance, and for every model order n_p, the signal $\tilde{x}_{est}(n_p)$ is estimated by SVD of $\boldsymbol{H}$ and recomputing it using every n_p number of singular vectors and singular values. The order for which the error between true and recomputed data matrix is minimal, corresponds to the model order R. In order to determine the robustness of the model order estimation, the whole estimation process can be repeated for a finite number of iterations, with different perturbations every iteration. The reason behind the deployment of SVD to predict the signal will become obvious in Section VI.

With the estimated model order R, the multiplicities are selected from a set of possibilities. For $R = 3$, the possible multiplicities are $M_k = \{(1,1,1), (1,2), (2,1), (3)\}$. The multiplicities of poles, estimated by any estimation method, should match one of the possibilities from the set. However, in practice, all estimated signal poles appear as simple poles, due to the perturbation.

V-B. Estimation of Complex Amplitude

The complex amplitude estimates $\hat{c}_k$, $k = 1, ...R$ are obtained by solving equation (25) by least square method, where $\boldsymbol{T}$ is $N \times R$ modified-confluent Vandermonde matrix.

$$\boldsymbol{T}\boldsymbol{c} = \boldsymbol{x_n}, \quad n = 0, 1, ..., N-1, \tag{25}$$

where $\boldsymbol{c}$ is a vector of length R containing complex amplitudes estimates and $\boldsymbol{x_n}$ is length N signal vector. The modified-confluent Vandermonde matrix $\boldsymbol{T}$ introduced in this work is similar to Pascal-Vandermonde matrix in [12] or confluent Vandermonde matrix in [13], where the j^{th} column, $j = 2, ..., M_k, k = 1, ..., r$ is a scaled $(j-1)^{\text{th}}$ derivative of the first column.

For model order, $R = 4$ and number of distinct poles, $r = 1$ with multiplicity $M_1 = 4$, $\boldsymbol{T}$ is given as:

$$\boldsymbol{T} = \begin{bmatrix} \hat{z}_1^n & n\hat{z}_1^n & n^2\hat{z}_1^n & n^3\hat{z}_1^n \end{bmatrix}, \quad n = 0, 1, ..., N-1.$$

$$\boldsymbol{T} = \begin{bmatrix} 1 & 0 & 0 & 0 \\ \hat{z}_1 & \hat{z}_1 & \hat{z}_1 & \hat{z}_1 \\ \vdots & \vdots & \vdots & \vdots \\ \hat{z}_1^t & t\hat{z}_1^t & t^2\hat{z}_1^t & t^3\hat{z}_1^t \end{bmatrix},$$

where $t = N-1$. The amplitude $\hat{a}_k$ and phase $\hat{\phi}_k$ estimates are then computed from vector $\boldsymbol{c}$, as shown in (27) and (28).

$$\hat{c}_k = \hat{a}_k e^{j\hat{\phi}_k}, \tag{26}$$

$$\hat{a}_k = \sqrt{\Re(\hat{c}_k)^2 + \Im(\hat{c}_k)^2}, \tag{27}$$

$$\hat{\phi}_k = \arctan\left(\frac{\Im(\hat{c}_k)}{\Re(\hat{c}_k)}\right), \tag{28}$$

(28) works only when $\frac{-\pi}{2} < \hat{\phi}_k < \frac{\pi}{2}$. Thus, (29) is valid for $-\pi < \hat{\phi}_k < \pi$, as given in [12]:

$$\hat{\phi}_k = -2\arctan\left(\frac{\Im(\hat{c}_k)}{\hat{a}_k + \Re(\hat{c}_k)}\right), \tag{29}$$

where $\Re(\hat{c}_k)$ and $\Im(\hat{c}_k)$ are real and imaginary parts of $\hat{c}_k$.

V-C. Equivalence between the parametrization of Proposed and PACE Models

The poles of the proposed (8) and the PACE (9) models are equal, but their complex amplitudes form a proportionality, that can be derived. The matrix forms of proposed and PACE model are given by (30) and (31) respectively.

$$\tilde{\boldsymbol{T}}\tilde{\boldsymbol{c}} = \tilde{\boldsymbol{x}}_{\boldsymbol{n}}, \quad n = 0, 1, ..., N-1 \tag{30}$$

$$\boldsymbol{T'c'} = \boldsymbol{x'_n}, \quad n = 0, 1, ..., N-1 \tag{31}$$

Equating the matrix forms of the two models, since the signal sequences $\tilde{\boldsymbol{x}}_{\boldsymbol{n}}$ and $\boldsymbol{x'_n}$ are equal, we get:

$$\tilde{\boldsymbol{T}}\tilde{\boldsymbol{c}} = \boldsymbol{T'c'} \tag{32}$$

The matrices $\tilde{\boldsymbol{T}}$ and $\boldsymbol{T'}$ are confluent, and so are the vectors $\tilde{\boldsymbol{c}}$ and $\boldsymbol{c'}$, each segment representing one signal pole. Expanding the equation (32), we get:

$$\begin{bmatrix}\tilde{\boldsymbol{T}}_{\boldsymbol{1}} & \tilde{\boldsymbol{T}}_{\boldsymbol{2}} & \dots & \tilde{\boldsymbol{T}}_{\boldsymbol{r}}\end{bmatrix}\begin{bmatrix}\tilde{\boldsymbol{c}}_{\boldsymbol{1}}\\ \tilde{\boldsymbol{c}}_{\boldsymbol{2}}\\ \vdots\\ \tilde{\boldsymbol{c}}_{\boldsymbol{r}}\end{bmatrix} = \begin{bmatrix}\boldsymbol{T'_1} & \boldsymbol{T'_2} & \dots & \boldsymbol{T'_r}\end{bmatrix}\begin{bmatrix}\boldsymbol{c'_1}\\ \boldsymbol{c'_2}\\ \vdots\\ \boldsymbol{c'_r}\end{bmatrix}. \tag{33}$$

Every individual block in $\boldsymbol{T'}$ is a lower triangular Pascal matrix, and inverting the confluent $\boldsymbol{T'}$ matrix will not preserve the structure. Moreover, the contributions to complex amplitudes in a block are dependent only on the poles of the corresponding block. Thus, the inversion can be performed blockwise. The complex amplitudes of the k^{th} pole are:

$$\boldsymbol{c'_k} = \boldsymbol{T'_k}^{-1}\tilde{\boldsymbol{T}}_{\boldsymbol{k}}\tilde{\boldsymbol{c}}_{\boldsymbol{k}}. \tag{34}$$

Since $\boldsymbol{T'_k}$ has lower triangular Pascal structure, so is its inverse $\boldsymbol{T'_1}^{-1}$. Let $s = M_K - 1$, then

$$\boldsymbol{T'_k} = \begin{bmatrix}1 & & & & & \\ 1 & 1/z_k & & & & \\ 1 & 2/z_k & 1/z_k^2 & & & \\ 1 & 3/z_k & 3/z_k^2 & 1/z_k^3 & & \\ \vdots & & & & \ddots & \\ 1 & \dots & \dots & \dots & \dots & 1/z_k^s\end{bmatrix},$$

$$\boldsymbol{T'_k}^{-1} = \begin{bmatrix}1 & & & & & \\ -z_k & z_k & & & & \\ z_k^2 & -2z_k^2 & z_k^2 & & & \\ -z_k^3 & 3z_k^3 & -3z_k^3 & z_k^3 & & \\ \vdots & & & & \ddots & \\ -1^{i+j}z_k^s & \dots & \dots & \dots & \dots & z_k^s\end{bmatrix}.$$

$$\boldsymbol{T'_k}^{-1} = \begin{cases}-1^{i+j}\binom{i}{j}z^i = \dfrac{-1^{i+j}i!z^i}{(i-j)!j!}, & \text{if } j \le i,\\ 0, & \text{otherwise,}\end{cases} \tag{35}$$

where $i, j = 0, ..., s$ are local positional indices of k^{th} block. Left-multiplying $\tilde{\boldsymbol{T}}_{\boldsymbol{k}}$, a dense matrix, with $\boldsymbol{T'_k}^{-1}$, an upper triangular matrix is formed, where the elements form an interesting series of a sum of binomial coefficients (38). The resulting upper triangular matrix (say $\boldsymbol{S}$) establishes the relationship between the complex amplitudes of both models.

$$\boldsymbol{T'_k}^{-1}\begin{bmatrix}1 & 0 & 0 & \dots & 0\\ 1 & 1 & 1 & \dots & 1\\ 1 & 2 & 4 & \dots & 2^s\\ \vdots & \vdots & \vdots & \vdots & \vdots\\ 1 & \dots & \dots & \dots & i^s\end{bmatrix}\begin{bmatrix}\tilde{c}_{11}\\ \tilde{c}_{12}\\ \vdots\\ \tilde{c}_{1M_k}\end{bmatrix} = \begin{bmatrix}c'_{11}\\ c'_{12}\\ \vdots\\ c'_{1M_k}\end{bmatrix}. \tag{36}$$

$$\begin{bmatrix}1 & 0 & 0 & 0 & \dots & 0\\ & z_k & z_k & z_k & \dots & z_k\\ & & 2!z_k^2 & 6z_k^2 & \dots & \vdots\\ & & & 3!z_k^3 & \dots & \vdots\\ & & & & \ddots & \vdots\\ & & & & & s!z_k^s\end{bmatrix}\begin{bmatrix}\tilde{c}_{11}\\ \tilde{c}_{12}\\ \vdots\\ \tilde{c}_{1M_k}\end{bmatrix} = \begin{bmatrix}c'_{11}\\ c'_{12}\\ \vdots\\ c'_{1M_k}\end{bmatrix}. \tag{37}$$

$$\boldsymbol{S} = \begin{cases}\left(\sum_{q=1}^{i} -1^{i+q}\binom{i}{q}q^j\right)z^i, & \text{if } i \le j,\\ 0, & \text{otherwise,}\end{cases} \tag{38}$$

where $i, j = 1, ..., s$ and the first row and column of $\boldsymbol{S}$ are unit vectors, with unity in the first position. The proportionality between the complex amplitudes of k^{th} pole of both models is defined as:

$$\sum_{l=i+1}^{M_k}\left[\left(\sum_{q=1}^{i} -1^{i+q}\binom{i}{q}q^j\right)z^i\right]\tilde{c}_{kl} = c'_{kl}. \tag{39}$$

It is to be noted that the first complex amplitudes of every pole of both models are the same (i.e.) $\tilde{c}_{k1} = c'_{k1}$.

VI. INFLUENCE OF L ON ESTIMATES

The effect of Hankel matrix size, L, on the performance of the subspace-based methods has been studied, and optimal size for better estimates is proposed in this section.

The study is conducted for a discrete-time signal $\tilde{x}_n$ in (8), sample size $N = [500, 1000]$, $r = 1$ damped exponential with multiplicity $M_1 = R = 3$, input parameters $f = 0.02$ Hz, $\alpha = 0.009, a = [1, 4, 6] \times 1e-3, \phi = [0.1, 0.25, 0.5] \times \pi$ and $\Delta t = 1$, contaminated by circularly symmetric WGN b_n.

The parameters $L, M \in [R+1, N-R]$ since L and M should be greater than R at least by 1. A Monte-Carlo simulation, consisting of $N_{runs} = 100$ independent trial

runs, is performed. The parameter estimates in Fig. 2 are formulated in terms of averaged RMS error (RMSE).

$$RMSE(q_k) = \sqrt{\frac{1}{N_{runs}} \sum_{i=1}^{N_{runs}} (\hat{q}_{k,i} - q_k)^2}, \qquad (40)$$

where q_k is the k^{th} value of a true parameter: f, α, a or ϕ and $\hat{q}_{k,i}$ is the k^{th} estimate of corresponding parameter for the i^{th} trial run of N_{runs} Monte-Carlo simulation. The averaged RMS error of the parameter q is given as $\overline{RMSE(q)}$:

$$\overline{RMSE(q)} = \frac{1}{R} \sum_{k=1}^{R} RMSE(q_k). \qquad (41)$$

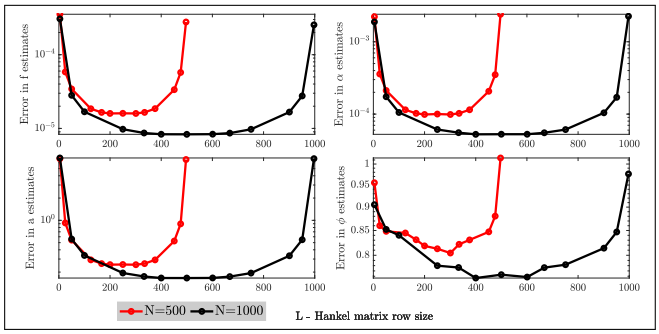

Fig. 2: Averaged RMSE of estimates vs. L for signal with triple pole, by HTLS, $N = 500$ (•), 1000 (•), SNR=120 dB. For $L \in [\frac{N}{3}, \frac{2N}{3}]$, the estimates are better. The symmetricity along L is because of the property of the Hankel matrix.

From Fig. 2, it is clear that the model parameter estimates are better, when the Hankel matrix is (nearly) square, i.e. $\frac{N}{3} \leq L_{optimal} \leq \frac{2N}{3}$. In case of noisy data matrices, for short-fat $\boldsymbol{H}$ i.e. $L \in [N+1, \frac{N}{3})$ and tall-skinny $\boldsymbol{H}$ i.e. $L \in (\frac{2N}{3}, N-R]$, the $rank(\boldsymbol{H}) = \min(L, M)$ is not sufficient for an efficient parameter estimation . For matrices in $L_{optimal}$ range, the rank is higher, and it is maximal for $L = N/2$ and $L = 1 + N/2$ (nearly square matrices). Hence, the estimates have better accuracy. The symmetric trend in the error of the estimates along the hyperparameter L is because the matrices of size $L \geq 1 + \frac{N}{2}$ are transpose of the matrices of size $L \leq \frac{N}{2}$, explaining that the SVD of these matrices are also transposed, and have same singular values. Although the (nearly) square Hankel matrices prove to be efficient in terms of accuracy, it is associated with higher computational cost in comparison to the short-fat and tall-skinny matrices as shown in Fig. 3. The higher computational cost can be explained by the two computationally expensive steps in subspace-based methods: namely SVD and TLS steps. In cases, where accuracy is more important than simulation time, L can be chosen between $\frac{N}{3}$ and $\frac{2N}{3}$.

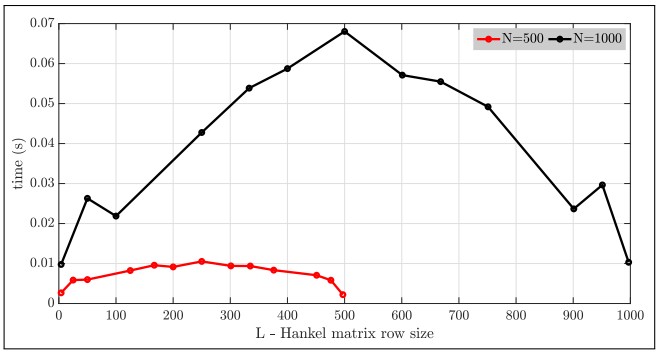

Fig. 3: Average time for 1 Monte-Carlo Simulation vs. L for signal with triple pole by HTLS, $N = 500$ (•), 1000 (•), SNR=120 dB. Due to the handling of a large number of elements in SVD and TLS, estimation is slower for $L = \frac{N}{2}$.

VII. NUMERICAL EXAMPLES

The algorithms are tested for the noise-free case in Section VII-A, where parameter estimation is expected to have a minimal error, and later with noise in Section VII-B. Then, in Section VII-C, a real-valued signal example from [12] is taken for comparison of PACE and proposed models.

VII-A. Noise-free Signal

For the same example in Section VI, one Monte-Carlo trial with $N = 1000$ samples is performed. The size of $\boldsymbol{H}$ for subspace-based methods is fixed as $L = \frac{N}{2}$, to obtain better accuracy, as explained in Section VI. The averaged RMSE of the estimates by all 3 methods is given in Tab. I. It can be inferred that the accuracy of poles estimated by subspace-based methods is better than the linear method, and so are the individual parameter estimates.

Table I: Averaged RMSE of estimates for noise-free signal. The poles estimated by the 3 estimation methods gives directly $\hat{f}, \hat{\alpha}$. Using the poles in Vandermonde matrix $\boldsymbol{T}$ and solving a system of linear equations, $\hat{a}, \hat{\phi}$ are obtained.

Method	$r = 1, R = 3, M_1 = 3$			
	$\hat{f}$	$\hat{\alpha}$	$\hat{a}$	$\hat{\phi}$
HTLS	1e-8	1e-7	1e-9	1e-7
Kung	1e-8	1e-7	1e-9	1e-7
Linear Prediction	1e-5	1e-4	1e-6	1e-4

VII-B. Signal with noise

The results from the noise-free simulation confirm that the parameters of the signal with multiple poles are estimated with good accuracy. Further, the implementation is simulated with noisy data for $N_{runs} = 100$ Monte-Carlo trials, with the same simulation setting as above. The results are shown in Fig. 4, where the averaged RMSE of parameter estimates are plotted against the SNR.

Clearly, the frequency and damping factor estimates of subspace-based methods are better than the linear prediction for all SNR, explaining that the SVD and TLS steps in subspace-based methods, result in better accuracy of pole estimation. The estimated poles are then used in $\boldsymbol{T}$, and upon solving (25), we estimate complex amplitudes. The amplitude and phase estimates of all three methods are in the comparable range for low SNR because the error in estimated poles is raised to increasing powers of $n = 0, ..., N-1$, in $\boldsymbol{T}$ and then it is inverted to obtain the solution, leading to numerical inaccuracies. But in the higher SNR range, there is a clear distinction between the subspace-based methods and linear prediction, because of the negligible error in pole estimates and low noise perturbation.

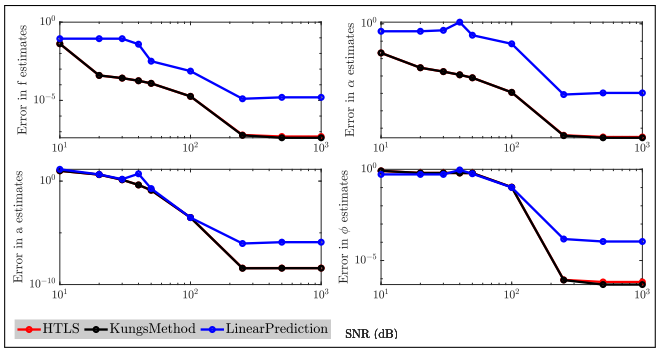

Fig. 4: RMSE of parameter estimates vs. SNR for $r = 1, M_1 = 3, f = 0.02$ Hz, $\alpha = 0.009, a = [1, 4, 6] \times 1e-3, \phi = [0.1, 0.25, 0.5] \times \pi$ by HTLS (●), Kung's method (●), Linear prediction (●). Subspace-based methods perform better than linear prediction because they are based on numerically stable SVD.

VII-C. Real-valued Signal with noise

This is a particular case of a real-valued signal example taken from [12], to compare the proposed and the PACE models [12]. If the prediction polynomial has real coefficients, then the roots/poles appear in real and complex conjugate pairs of the same multiplicity. Thus, the signal model (6) can be rewritten as below, by grouping the poles with the same absolute value of polar angles.

$$\tilde{s}[n] = \sum_{p=0}^{P-1} a_p[n] \cos(2\pi f_p n) + b_p[n] \sin(2\pi f_p n), \quad (42)$$

where $P \leq R$ is the number of distinct frequencies $f_p \in [0, 0.5]$, and $\forall p \in [0, ..., P-1]$, both $a_p[n]$ and $b_p[n]$ belong to a class of parametric functions of form (43), given in [12],

$$g[n] = \sum_{q=0}^{Q-1} P_q[n] e^{\alpha_q n}, \quad (43)$$

where P_q is a polynomial with real coefficients, $\forall q \in 0, ..., Q-1$, $Q \in \mathbb{N}^*$ (excludes 0) is the number of poles having the same polar angle, α_q are real and distinct damping factors. Then, the equation (42) is written as given in [12],

$$\tilde{s}[n] = \sum_{p=0}^{P-1} A_p[n] \cos(2\pi f_p n + \phi_p[n]). \quad (44)$$

The Amplitude and phase are time-dependent and they satisfy:

$$\begin{aligned} a_p[n] &= A_p[n] \cos(\phi_p[n]), \\ b_p[n] &= -A_p[n] \sin(\phi_p[n]). \end{aligned} \quad (45)$$

The solutions of $A_p[n], \phi_p[n]$ are the same as solutions of complex amplitude estimates given in Section V-B.

For a signal defined in (42) with $P = 1$, $f_0 = 0.0086$, $a_0[n] = \frac{n^2}{25000} - 1$, $b_0[n] = 0$, and WGN with $SNR = 20$ dB, the corresponding model parameters estimates are: $r = 2, R = 6, M_k = [3, 3]$. The chosen time range is, $n \in [-250, 250]$ and the Hankel matrix size for subspace-based methods is $L = M = 251$.

The poles in Fig. 5 are estimated by HTLS and generalized ESPRIT algorithm [12], where eigenvalue decomposition of correlation matrix $\boldsymbol{W}$ is used instead of SVD. It can be observed that the poles of the real-valued signal are complex conjugate pairs of estimated multiplicity $M_k = [3, 3]$

$$\boldsymbol{W} = \frac{1}{M} \boldsymbol{H}\boldsymbol{H}^H \quad (46)$$

Three poles with positive angles, for SNR 20,1000 dB,

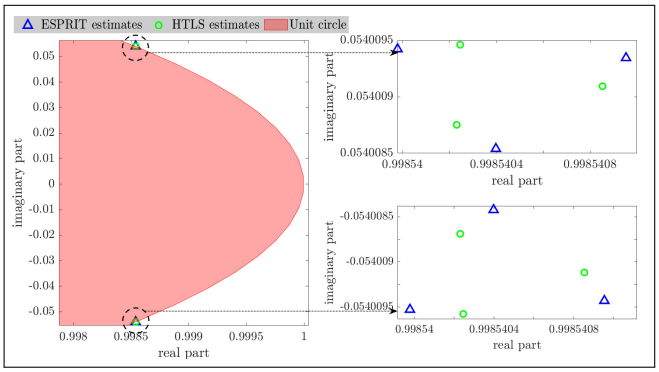

Fig. 5: Poles estimated by ESPRIT (△) and HTLS method (○) for SNR=1000 dB, appearing in complex conjugate pairs of multiplicity $M_K = [3, 3]$. The zoomed-in view of pole locations is shown on the right side. Right top - poles with positive angles, Right bottom - Poles with negative angles.

estimated by ESPRIT (△) and HTLS method (○) are plotted along with the true value (■) $z_0 = e^{i2\pi f_0}$ in Fig. 6. As discussed in [12], the poles are scattered as many simple poles, due to the first-order perturbation of z_0. Thus, the mean value of the estimated poles of ESPRIT and HTLS method (▲,●) are considered to be the closest approximation

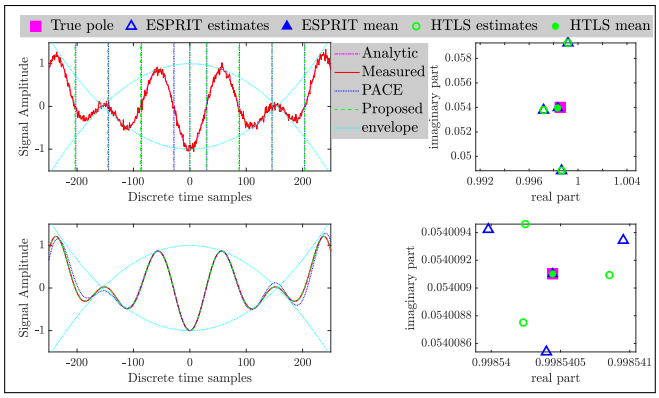

Fig. 6: Poles estimated by ESPRIT (△) and HTLS method (○) for SNR=$[20, 1000]$ dB, plotted along with corresponding means (▲,●) and the true pole location (■). The measured and predicted signal using the estimated parameters by PACE and proposed models are also plotted on the left side.

to the true pole.

It is observed that estimates by both subspace-based methods are almost close to each other. The pole estimates are used further to estimate the complex amplitudes by the proposed and the PACE models. With pole and complex amplitude estimates, the signal is re-computed by both models, and they are compared in Figs. 6, 7. The true signal is reproduced well with good accuracy for higher SNR, but with SNR=20 dB, the pole estimates are perturbed and that is further perturbed in the complex amplitude estimation.

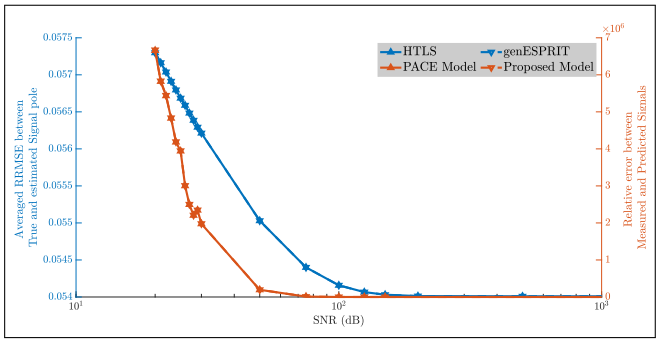

Fig. 7: Averaged relative RMSE between true and estimated poles by HTLS (▲) and generalized ESPRIT method (▼) for varying SNR. Relative error between the true signal and the signal predicted by PACE (▲) and proposed models (▼).

The following observations can be made:

- For a simple case: a single pole repeating thrice, the estimates are good and improve with increasing SNR. The estimates by subspace-based methods are approximately the same, because their procedures are similar, by determining the left singular vector and singular values and then solving a linear system of equations with the shift-invariance property.
- The estimates by linear prediction have high variance, because the computation of companion matrix $\boldsymbol{A}$ using the polynomial coefficients $p1, ..., p_R$ is unstable, and so the pole estimates $\hat{z}_k$, $k = 1, ..., R$ computed thereafter.
- The error in estimation increases for increasing order and multiplicity, because the signal computed from true parameters is numerically unstable with increasing multiplicity, as the polynomial times exponential function leads to signal overshoot. This issue can be circumvented by using low true parameter values for amplitude. But it is not a practical solution. Thus, the inverse modelling of a system with a multiplicity of poles 3 or lower, can be successful with the model presented in (8). The multiple poles appear as multiple simple poles within a small circle of radius ϵ and with the true pole as the centre. The estimated poles form a regular polygon of sides equal to its multiplicity.
- The estimates are not necessarily in the same order as they were input in the system (in cases where parameters are fed into the system and recomputed). This might lead to an increased error. To avoid such unforeseen errors, it is recommended to input the true parameters in an ordered fashion (ascending or descending).
- The model order and multiplicity estimation by AIC is influenced by increasing order, multiplicity and noise.
- The accuracy of pole estimates reduces with noise. The perturbed poles are used to estimate the complex amplitudes. Thus, the predicted signal for lower SNR has a higher variance. The deviation between the pole estimates of HTLS and the generalized ESPRIT method is very negligible, and so is the deviation between the predicted signals by PACE and the proposed model.

VIII. CONCLUSION

In this paper, a generalized model for signals with multiple poles was proposed. The estimates by subspace-based and linear methods were compared. The model order and multiplicity estimations were also proposed. The size of the data matrices in subspace-based methods played a significant role in the statistical accuracy of estimates, concluding that the optimal size of the data matrix should be between one-third and two-thirds of the sample size. The subspace-based methods resulted in better estimates, as they involve numerically stable SVD, while linear prediction estimated poles through the state matrix of the system, which is constructed by the coefficients determined from the recurrence relation of the polynomial function, leading to numerically unstable results. The pole multiplicity, model order and noise should be limited for better accuracy of estimation.

ACKNOWLEDGEMENT

IM received funding from FWO projects G090117N and G033822N and the FNRS–FWO EOS Project 30468160. KU Leuven start-up-grant STG/19/036 ZKD7924.

IX. REFERENCES

[1] Sircar, P.: Mathematical Aspects of Signal Processing, 2016, Delhi.

[2] Stoica, P., Sharmen, K.C.: Maximum likelihood methods for direction-of-arrival estimation. IEEE Trans. Acous., 1990, p. 1132–1143.

[3] Kumaresan, R., Tufts, D.W.: Estimating the Parameters of Exponentially Damped Sinusoids and Pole-Zero Modeling in Noise, IEEE Trans. of Acous., 1982, Vol. ASSP-30, No.6, p. 833-839.

[4] Bhaskar Rao, D.V., Arun, K.S.: Model-based processing of signals: a state-space approach. Proc. IEEE 1992, 80, p. 283–309.

[5] Kung, S.Y., Arun, K.S., Bhaskar Rao, D.V.: State-space and singular value decomposition-based approximation methods for the harmonic retrieval problem. J. Opt. Soc. Am. 1983, 73(12), p. 1799–1811.

[6] Markovsky, I., Vaccaro, R.J., Van Huffel, S.: System identification by optimal subspace estimation, Dept. EE, K.U.Leuven, 2006.

[7] Hua, Y., Sarkar, T.K.: Matrix pencil method for estimating parameters of exponentially damped/undamped sinusoids in noise. IEEE Trans. Acoust. 1990, 38, p. 814–824.

[8] Papy, J.-M., De Lathauwer, L., Van Huffel, S.: Exponential data fitting using multilinear algebra: the decimative case, Journal of Chemometrics 2009, DOI:10.1002/cem.1212, p. 341–351.

[9] Morren, G., Lemmerling, P., Van Huffel, S.: Decimative subspace-based parameter estimation techniques, Elsevier, Signal Processing 83, 2003, p. 1025 – 1033

[10] Markovsky, I.: Low-Rank Approximation, Algorithms, Implementation, Applications, 2018, ch.3, p. 72-75.

[11] Antoulas, A.C., Sorensen, D.C.: Approximation of Large-Scale Dynamical Systems: An Overview, International Journal of Applied Mathematics and Computer Science, 2001, Vol.11, No.5, p. 1093–1121.

[12] Roland, B., Bertrand, D., and Gaël, R.: High-resolution spectral analysis of mixtures of complex exponentials modulated by polynomials, IEEE Transactions on Signal Processing, April 2006, Vol. 54, No. 4.

[13] Franklin T.L., Sanzheng, Q., David, V.: Exponential Decomposition and Hankel Matrix, Mathematics in Signal Processing V: Based on the Proceedings of a Conference, 2000, p. 275-285.

[14] Riche de Prony, G. M.: Essai expérimental et analytique: sur les lois de la dilatabilité de fluides élastiques et sur celles de la force expansive de la vapeur de l'eau et de la vapeur de l'alcool à différentes températures, Journal de l'école polytechnique, Vol. 1, no. 22, pp. 24–76, 1795, in French.

[15] Pisarenko, V. F.: The retrieval of harmonics from a covariance function, Geophysical J. Royal Astron. Soc., Vol. 33, pp. 347–366, 1973.

[16] McNamee J.M.: Numerical Methods for Roots of Polynomials - Part I, Elsevier Science, Vol.14, 1st edition - June 4, 2007.